Phonons in low-dimensional systems

2001 J. Phys.: Condens. Matter 13 7611

(http://iopscience.iop.org/0953-8984/13/34/309)

INSTITUTE OF PHYSICS PUBLISHING JOURNAL OF PHYSICS: CONDENSED MATTER

J. Phys.: Condens. Matter **13** (2001) 7611–7626 PII: S0953-8984(01)24202-7

Phonons in low-dimensional systems

Jürgen Fritsch

Institut für Theoretische Physik, Universität Regensburg, D-93040 Regensburg, Germany

E-mail: juergen.fritsch@physik.uni-regensburg.de

Received 24 April 2001
Published 9 August 2001
Online at stacks.iop.org/JPhysCM/13/7611

Abstract

The surfaces of a crystal solid with a given crystallographic orientation are usually described by the two dimensions of their extension. In the case of well-defined periodicity, surface vibrational states are characterized by two-dimensional wavevectors with non-vanishing dispersion in all directions parallel to the surface. Microscopic processes such as rebonding of atoms and adsorption, however, can lead to structural units on a surface that show one- or even zero-dimensional signature. Phonon dispersion curves for clean and adsorbate-covered surfaces of Si and III–V compounds are computed by means of density-functional perturbation theory in the framework of slab-lattice dynamics. These systems show surface phonon modes that clearly have two-, one-, and zero-dimensional character. Vibrational states, which are obvious fingerprints of their structural origin on the surface, are discussed in detail.

(Some figures in this article are in colour only in the electronic version)

1. Introduction

Surface phonon modes are, generally speaking, vibrational excitations, in which the displacements of atoms are large near the surface and decrease essentially exponentially into the bulk. The investigation of localized phonon modes therefore provides information about the atomic geometry, bonding structure, and the interatomic force constants in the topmost layers of a solid. Semiconductor surfaces are particularly interesting, because of the covalent bonding forces in the substrate. The break-up of directed bonds on the surface often results in the formation of new bonding units and charge redistribution from energetically higher to more favourable electronic states. Such processes can lead to the creation of lower-dimensional structures in the surface region. Typical examples for one-dimensional objects are the zigzag chains on the (110) surfaces of free and Sb-covered III–V compound semiconductors (see figure 8 below) and the dimer rows on the Si(001) surface (see figure 10 below). Direct observation of these linear features was achieved by means of scanning tunnelling microscopy (STM) [1, 2].

0953-8984/01/347611+16$30.00

The adsorption of small atoms can lead to a situation where the coupling of the chemisorbed atoms with the substrate is much stronger than the interaction between the atoms of the adlayer. In such cases, the vibrations of the chemisorption layer are mainly determined by the on-site coupling. Hence, the adsorbed atoms can be considered as uncoupled oscillators, especially if the mass of the substrate atoms is significantly larger than that of the adatoms. A typical example for vibrational states with zero-dimensional character is the adatom stretching mode of the Si(111) surface covered with one monolayer (ML) of hydrogen (see figure 5 below).

Supported by the remarkable advances achieved in the development of computational schemes based on density-functional theory (DFT) [3,4] and the availability of supercomputers, it is now possible to determine complete phonon dispersion curves for the bulk and the surfaces of crystal solids within *ab initio* calculations that are free from any adjustable parameters. The results presented in this paper were calculated in the framework of density-functional perturbation theory (DFPT) [5,6], which is described in detail in the contribution of Pavone [7]. With this method, it is possible to compute in a consistent way the atomic equilibrium positions, charge redistribution, bonding, and the phonon dispersion of free and adsorbate-covered semiconductor surfaces.

The paper is organized as follows. Section 2 gives an introduction to the concept of slab-lattice dynamics and the terminology generally used to describe crystal surfaces and their phonon modes. Section 3 is focused on the Si(111) surface covered by hydrogen and group-III atoms. These systems show quasi-zero-dimensional vibrational modes. In section 4, structures with one-dimensional behaviour are discussed. The chosen examples are Sb atoms adsorbed on the (110) surfaces of III–V compounds and the dimer rows on Si(001). Section 5 addresses the majority surface vibrational states which have by nature two-dimensional character. The paper is summarized in section 6.

2. Surfaces and slab-lattice dynamics

While a few bulk phonon dispersion curves have been determined by means of inelastic x-ray scattering, this has not yet been done for surface modes. In a macroscopic view, surfaces can be described as two-dimensional planes at which a solid terminates. Because of atomic rearrangements and charge redistribution, it is necessary, however, to consider a sufficiently large surface region which comprises all atomic layers that are affected by the truncation of the solid. The orientation and the periodicity of a crystal surface are usually represented in the following form:

$$\text{material } (hkl)\ Z\ (m_1 \times m_2)\ \mathrm{R}\varphi.$$

The orientation of the surface is given by the Miller indices (hkl) of the bulk. There are primitive and centred surface structures which are reflected by $Z = \mathrm{p}$ and $Z = \mathrm{c}$, respectively. The numbers m_1 and m_2 indicate whether the surface has the same periodicity as the corresponding bulk (hkl) planes ($m_1, m_2 = 1$) or not. Primitive translations of increased length ($m_1 > 1$ or $m_2 > 1$) and eventually rotated orientation ($\mathrm{R}\varphi$) are needed to describe the translational symmetry of reconstructed surfaces. Reconstruction can result from the formation of new bonds, the removal of surface atoms, low-coverage adsorption, or other processes.

2.1. Thin crystal films

The bulk of crystal solids is usually described by primitive translations $\boldsymbol{a}_1$, $\boldsymbol{a}_2$, and $\boldsymbol{a}_3$ defining the Bravais lattice and the vectors $\boldsymbol{R}_\alpha^{\mathrm{bulk}}$ ($\alpha = 1, \ldots, n_{\mathrm{bulk}}$) giving the basis positions of all n_{bulk} atoms in the unit cell relative to its origin. Periodic repetition of the primitive unit cell

generates the entire crystal. The time-dependent position vector of an atom in the solid is represented by

$$\boldsymbol{R}'_{l\alpha}(t) = \boldsymbol{R}_{l\alpha} + \boldsymbol{u}_{l\alpha}(t) \tag{1}$$

where $\boldsymbol{u}_{l\alpha}(t)$ is the displacement of the αth atom in the $\boldsymbol{l}$th unit cell ($\boldsymbol{l} = (l_1, l_2, l_3)$) from the equilibrium position

$$\boldsymbol{R}_{l\alpha} = \boldsymbol{R}_l + \boldsymbol{R}_\alpha^{\text{bulk}} = l_1\boldsymbol{a}_1 + l_2\boldsymbol{a}_2 + l_3\boldsymbol{a}_3 + \boldsymbol{R}_\alpha^{\text{bulk}}. \tag{2}$$

The integers l_1, l_2, and l_3 range in the interval from $-\infty$ to $+\infty$ for the bulk. With an appropriate choice of $\boldsymbol{a}_1$ and $\boldsymbol{a}_2$ *parallel to the surface*, a semi-infinite crystal with one surface can be represented by $-\infty < l_1 < +\infty$, $-\infty < l_2 < +\infty$, and $-\infty < l_3 \leqslant 0$ or $0 \leqslant l_3 < +\infty$.

Surfaces are more conveniently described on the basis of thin crystal films which comprise a sufficiently large (but finite) number of atomic layers with infinite extension in the plane of the slabs. The lattice vectors

$$\overline{\boldsymbol{R}}_{\bar{l}} = l_1\boldsymbol{a}_1 + l_2\boldsymbol{a}_2 \tag{3}$$

form a two-dimensional lattice in the (x, y) plane with vanishing z-component as indicated by the abbreviations

$$\overline{\boldsymbol{R}} = (R_1, R_2, 0) \qquad \text{and} \qquad \bar{\boldsymbol{l}} = (l_1, l_2, 0). \tag{4}$$

The atomic equilibrium positions in the crystal film are defined by

$$\boldsymbol{R}_{\bar{l}\alpha} = \overline{\boldsymbol{R}}_{\bar{l}} + \boldsymbol{R}_\alpha \tag{5}$$

where the basis vectors $\boldsymbol{R}_\alpha$ specify the positions of all atoms in the slab unit cell. The index α indicates the type of atom and the layer of the crystal film in which it resides. Typically, slab unit cells used in electronic structure calculations comprise about ten atomic layers. The primitive translations $\boldsymbol{a}_1$ and $\boldsymbol{a}_2$ correspond to the lattice constant determined for the bulk material and have to be chosen in accord with the reconstruction of the surface. The primitive translations $\boldsymbol{b}_1$ and $\boldsymbol{b}_2$ of the reciprocal space are defined according to the relations

$$\boldsymbol{b}_1 = 2\pi\frac{\boldsymbol{a}_2 \times (\boldsymbol{a}_1 \times \boldsymbol{a}_2)}{|\boldsymbol{a}_1 \times \boldsymbol{a}_2|^2} \qquad \text{and} \qquad \boldsymbol{b}_2 = 2\pi\frac{\boldsymbol{a}_1 \times (\boldsymbol{a}_2 \times \boldsymbol{a}_1)}{|\boldsymbol{a}_1 \times \boldsymbol{a}_2|^2}. \tag{6}$$

Figure 1 illustrates the two-dimensional Brillouin zones of the most commonly investigated zincblende-compound semiconductor surfaces. The (001) and (111) surfaces of elemental semiconductors often exhibit (2×1) reconstructions as indicated in the lower part of figure 1. For all cases, standard labels for high-symmetry points are given.

2.2. Slab-lattice dynamics

The adiabatic potential, which is the sum of all ion–ion interaction terms and the electronic ground-state energy, determines the vibrational properties of the crystal film. Its Taylor expansion has a vanishing first-order term for small atomic displacements $\{\boldsymbol{u}_{\bar{l}\alpha}\}$ from the equilibrium positions $\{\boldsymbol{R}_{\bar{l}\alpha}\}$ and is given by

$$V_{\text{ad}}(\{\boldsymbol{R}_{\bar{l}\alpha} + \boldsymbol{u}_{\bar{l}\alpha}\}) = V_{\text{ad}}(\{\boldsymbol{R}_{\bar{l}\alpha}\}) + \frac{1}{2}\sum_{\bar{l}\alpha i}\sum_{\bar{l}'\alpha' j}\Phi_{ij}(\bar{l}\alpha, \bar{l}'\alpha')u_{\bar{l}\alpha i}u_{\bar{l}'\alpha' j} + \cdots. \tag{7}$$

The indices i and j denote the three Cartesian coordinates. The coefficients $\Phi_{ij}(\bar{l}\alpha, \bar{l}'\alpha')$ are the harmonic force constants defined as the second-order derivatives of the adiabatic potential with respect to the atomic displacements taken in the positions of minimal energy ($\{\boldsymbol{u}_{\bar{l}\alpha}\} = 0$):

$$\Phi_{ij}(\bar{l}\alpha, \bar{l}'\alpha') = \left.\frac{\partial^2 V_{\text{ad}}}{\partial u_{\bar{l}\alpha i}\,\partial u_{\bar{l}'\alpha' j}}\right|_{\{\boldsymbol{u}_{\bar{l}\alpha}\}=0}. \tag{8}$$

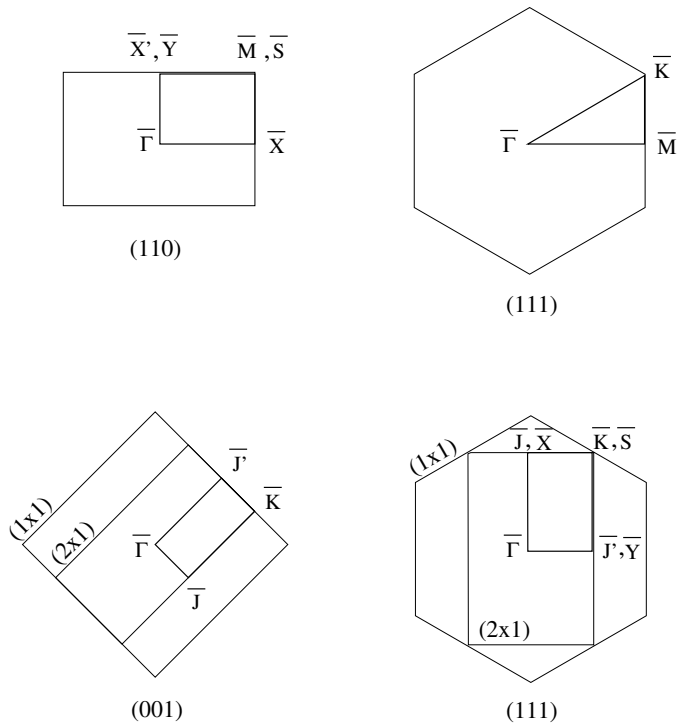

Figure 1. Surface Brillouin zones for the (110), (111), and (001) surfaces of zincblende-compound semiconductors. The lower part shows the Brillouin zones of (1×1) and (2×1) surface geometries.

In the harmonic approximation, the equations of motion for the atomic displacements can be written as

$$M_\alpha \frac{\mathrm{d}^2}{\mathrm{d}t^2} u_{\bar{l}\alpha i} = -\sum_{\bar{l}'\alpha' j} \Phi_{ij}(\bar{l}\alpha, \bar{l}'\alpha') u_{\bar{l}'\alpha' j} \tag{9}$$

where M_α is the mass of the αth atom in the unit cell.

Translational periodicity is assumed parallel to the surface for all planes of the crystal film. We therefore search for solutions of the equations of motion (9) in the form

$$u_{\bar{l}\alpha i} = \frac{1}{\sqrt{M_\alpha}} v_{\alpha i}(\overline{q}) \mathrm{e}^{\mathrm{i}(\overline{q}\cdot\overline{R}_{\bar{l}} - \omega t)} \tag{10}$$

where $\overline{q} = (q_1, q_2, 0)$ is a wavevector lying in the surface Brillouin zone. Substitution of equation (10) into equation (9) yields the eigenvalue problem

$$\omega^2(\overline{q}) v_{\alpha i}(\overline{q}) = \sum_{\alpha' j} \mathbf{D}_{ij}(\alpha\alpha', \overline{q}) v_{\alpha' j}(\overline{q}) \tag{11}$$

with the dynamical matrix defined by

$$\mathbf{D}_{ij}(\alpha\alpha', \overline{q}) = \sum_{\bar{l}'} \frac{1}{\sqrt{M_\alpha M_{\alpha'}}} \Phi_{ij}(\bar{l}\alpha, \bar{l}'\alpha') \mathrm{e}^{-\mathrm{i}\overline{q}\cdot(\overline{R}_{\bar{l}} - \overline{R}_{\bar{l}'})}. \tag{12}$$

For n atoms in the slab unit cell the dynamical matrix has the dimension $(3n \times 3n)$. Diagonalization of the Hermitian matrix for each wavevector $\overline{q}$ in the SBZ yields $3n$ real and non-negative eigenvalues $\omega_{\mathrm{s}}^2(\overline{q})$ and $3n \times 3n$ eigenvector components $v_{\alpha i}^{\mathrm{s}}(\overline{q})$.

The $3n$ normal modes of the slab determined for each $\overline{q}$ can be classified with respect to their polarization and the square of the amplitudes in the different layers of the crystal film. Bulk and surface modes are distinguished according to the behaviour of their amplitude as a function of the layer depth. While bulk modes do not change significantly in vibrational amplitude when comparing the outer with the inner planes of the slab, the atomic displacements associated with true surface vibrations decrease essentially exponentially approaching the central layers of the crystal film. Resonances result from a mixing of true surface modes with phonon states of the bulk. Their vibrational amplitude does not decay approaching the inner region; however, it exhibits larger components in the surface layers.

2.3. Slab dispersion relations

The eigenfrequencies $\omega_s(\overline{q})$ are usually plotted as a function of the wavevector $\overline{q}$. Typical slab dispersion relations comprise all branches ($s = 1, \ldots, 3n$). The majority of the $3n$ branches represent bulk-like phonon modes. Only a small number are related to localized and resonant surface vibrations. While the number of surface phonon modes is characteristic and does not change with the size of the crystal film, the number of bulk-related branches increases as more atomic layers are used in the slab calculation. All bulk-related branches lie in a frequency range determined by the vibrational spectrum of the material. In slab calculations the bulk phonon dispersion perpendicular to the plane of the crystal film is effectively folded back to a corresponding wavevector $\overline{q}$ in the SBZ. This results from the fact that the number of layers per crystal film is usually much larger compared to the minimum number required to describe the bulk using the same lattice vectors $\boldsymbol{a}_1$, $\boldsymbol{a}_2$ as for the surface (*slab-adapted bulk*). This is schematically illustrated in figure 2 for the bulk phonon dispersion of InP folded onto wavevectors lying in the (110) plane.

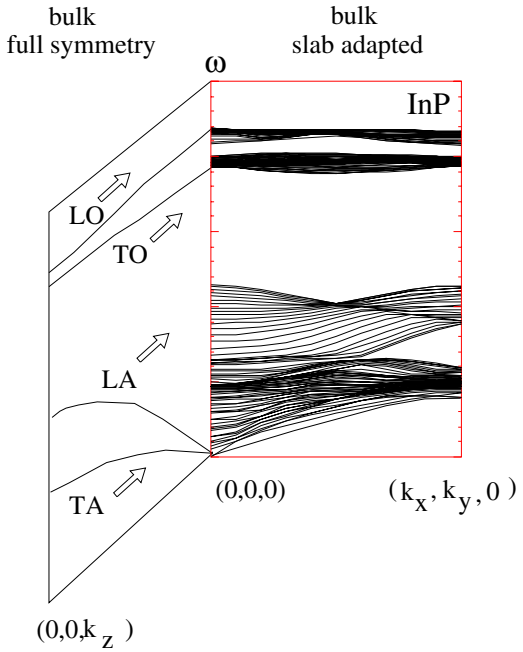

Figure 2. A schematic illustration of the projection of the bulk band structure of InP onto the (110) plane in the $\overline{\Gamma X}$ direction of the SBZ. The surface normal is oriented in the z-direction.

Bulk phonon branches appear in the entire range of the surface-projected band structure. The density of bulk branches is the greater the more atomic layers the single slab comprises. Gaps often appear in the bulk mode spectrum, especially for wavevectors $\overline{q}$ different from zero. No bulk vibration is allowed in such regions. Similarly to the case for InP, many diatomic crystals exhibit a gap between the acoustic and optical bulk modes for all wavevectors of the Brillouin zone. The existence of such gaps is interesting, since surface vibrations can occur in regions forbidden for bulk modes. This can be seen from the phonon dispersion of InP(110) which is shown in figure 3 for the $\overline{\Gamma X}$ direction. In such a case, surface phonons are well localized in the outer layers. True surface vibrational states can also occur in bulk mode frequency regions as long as the surface mode eigenvector has different symmetry to the eigenvectors of the phonons of the bulk with close-lying frequencies.

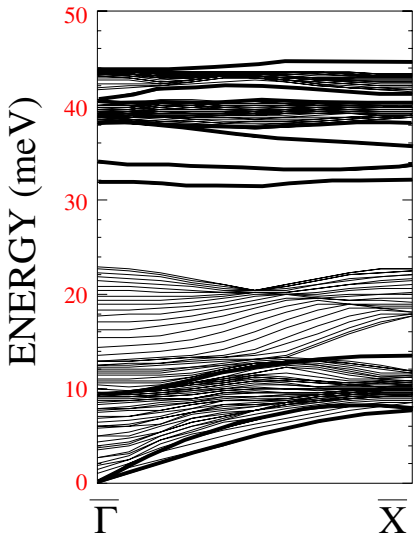

Figure 3. Phonon dispersion along the $\overline{\Gamma X}$ direction of a InP(110) slab comprising 25 atomic layers. Surface-localized states are indicated by thick lines, while all other vibrational states of the crystal film are represented by thin lines.

3. Phonon modes with zero-dimensional signature

The adsorbate-covered (111) surface of Si is an ideal system in which to study phonon modes with zero-dimensional character. The simplicity of the chemisorption structures is related to the bonding symmetry of the bulk material (see figure 4). The singly occupied dangling bonds of the bulk-terminated surface are ideal adsorption sites for hydrogen atoms or group-III atoms. Hydrogen adsorbs on top of each first-layer Si atom saturating all dangling bonds. It is possible to reach the 1 ML coverage limit [8], where the resulting H:Si(111)(1×1) surface has the same translational symmetry as the bulk planes. Because of their three valence electrons, group-III atoms adsorb on top of three first-layer Si atoms saturating their dangling bonds. The adsorption layer forms a hexagonal lattice, which can be described in terms of III:Si(111)$(\sqrt{3} \times \sqrt{3})$R30°. This means that the primitive translations of the group-III adlayer are rotated by 30° and increased in length by a factor of $\sqrt{3}$ with respect of those of the bulk (111) planes.

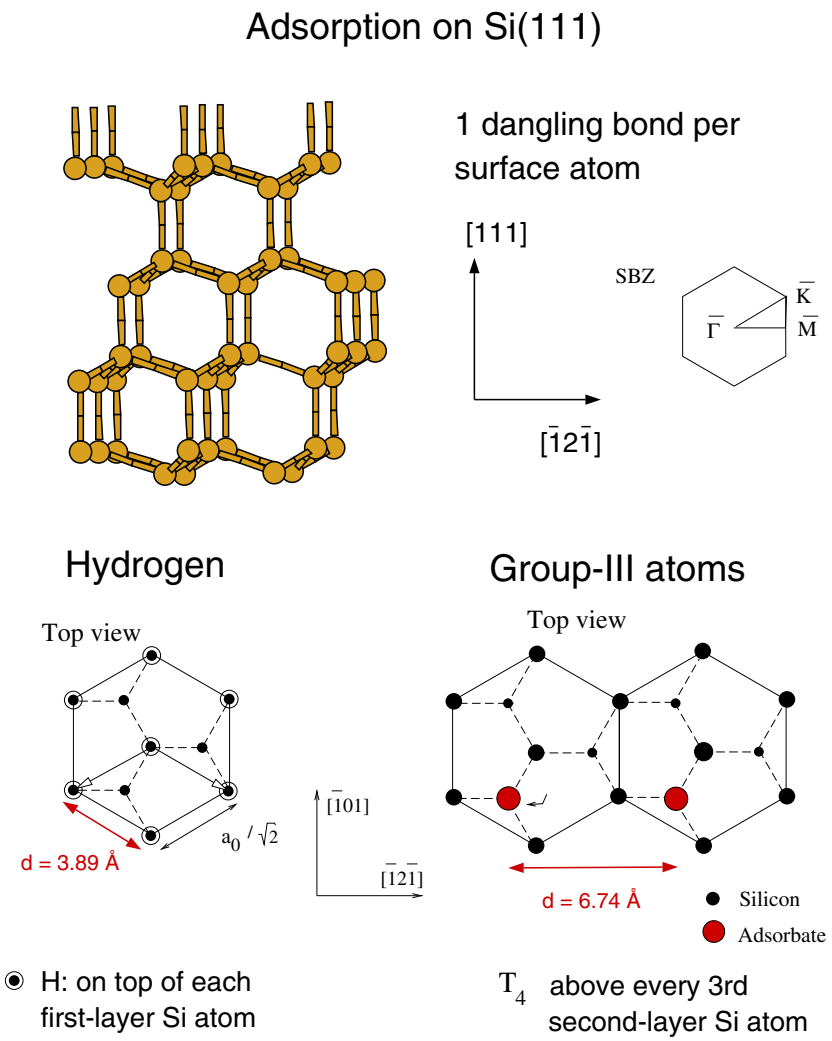

Figure 4. Adsorption of hydrogen and group-III atoms on the Si(111) surface. The first-layer atoms on the ideal Si(111) surface have one dangling bond normal to the surface. Hydrogen adsorbs on top of each first-layer Si atom saturating all dangling bonds. Group-III atoms adsorb at T_4 sites directly above second-layer atoms. The chemisorbed atoms are bonded to three first-layer Si atoms saturating their dangling bonds.

3.1. Hydrogen adsorption on Si(111)

As illustrated in figure 4, hydrogen atoms adsorbed on Si(111) form a hexagonal overlayer with an H–H distance of 3.89 Å. The H–H interaction is much weaker than the on-site coupling of each H atom, which can be described by one bond-stretching and two bond-bending force constants. The atomic mass of H is small compared with that of the substrate atoms. Therefore, substrate-mediated H–H coupling is also very weak.

Figure 5 illustrates the phonon dispersion computed for H:Si(111) along the $\overline{\Gamma M}$, $\overline{MK}$, and $\overline{K\Gamma}$ directions of the SBZ [9]. The flat branch at about 265 meV is the H stretching mode, which has a dispersion of only 0.7 meV. Hence, the frequency of this vibrational state is almost

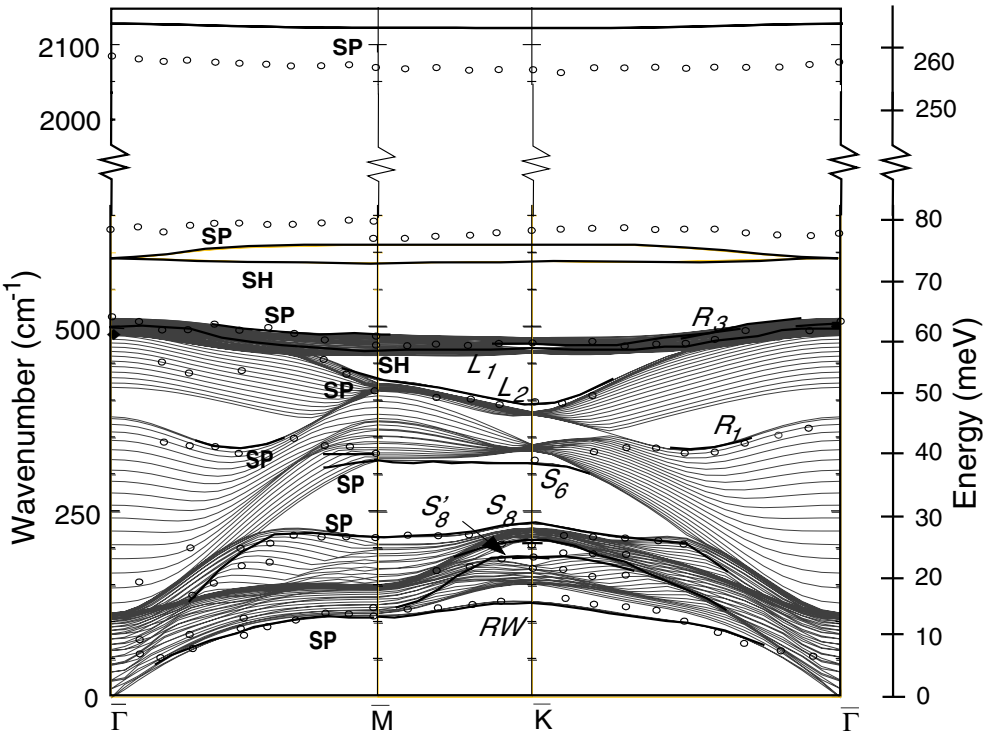

Figure 5. Phonon dispersion of H:Si(111). The vibrations of the adsorbed atoms are found above the energy range of all other phonons at about 265 meV (stretching mode) and 72 meV (bending modes). Experimental data from high-resolution electron energy-loss spectroscopy [10] are illustrated by the circles.

the same, irrespective of whether neighbouring atoms oscillate in phase or out of phase. This clearly shows that the interaction between neighbouring H atoms is weak. The bending modes have an energy of about 72 meV. They are degenerate at the $\overline{\Gamma}$ point—however, split into two separate branches with a dispersion of about 2.5 meV. This illustrates that the hydrogen atoms interact weakly when moving parallel to the surface. In contrast with the adlayer vibrations, the majority of surface phonon modes shown in figure 5 have two-dimensional character with appreciable dispersion in all directions.

3.2. Adsorption of group-III elements on Si(111)

The deposition of Al, Ga, and In on Si(111) leads to the formation of $(\sqrt{3} \times \sqrt{3})$R30° superstructures. STM experiments clearly show that chemisorbed Al and Ga atoms are bonded to Si(111) in positions above atoms of the second substrate layer [11–13] as illustrated in the lower part of figure 6. The bonds between the atoms 2 and 3 are compressed as a result of the adsorption. The phonon dispersion computed for Ga:Si(111)$(\sqrt{3} \times \sqrt{3})$R30° [14] is illustrated in the upper part of the figure. Most of the features recorded by means of inelastically scattered electrons and helium atoms can be attributed to localized surface states identified in the density-functional calculation.

Because of the large mass of the adsorbed atoms, there is no high-frequency stretching mode comparable to that of the H:Si(111) surface. A prominent feature in the measured

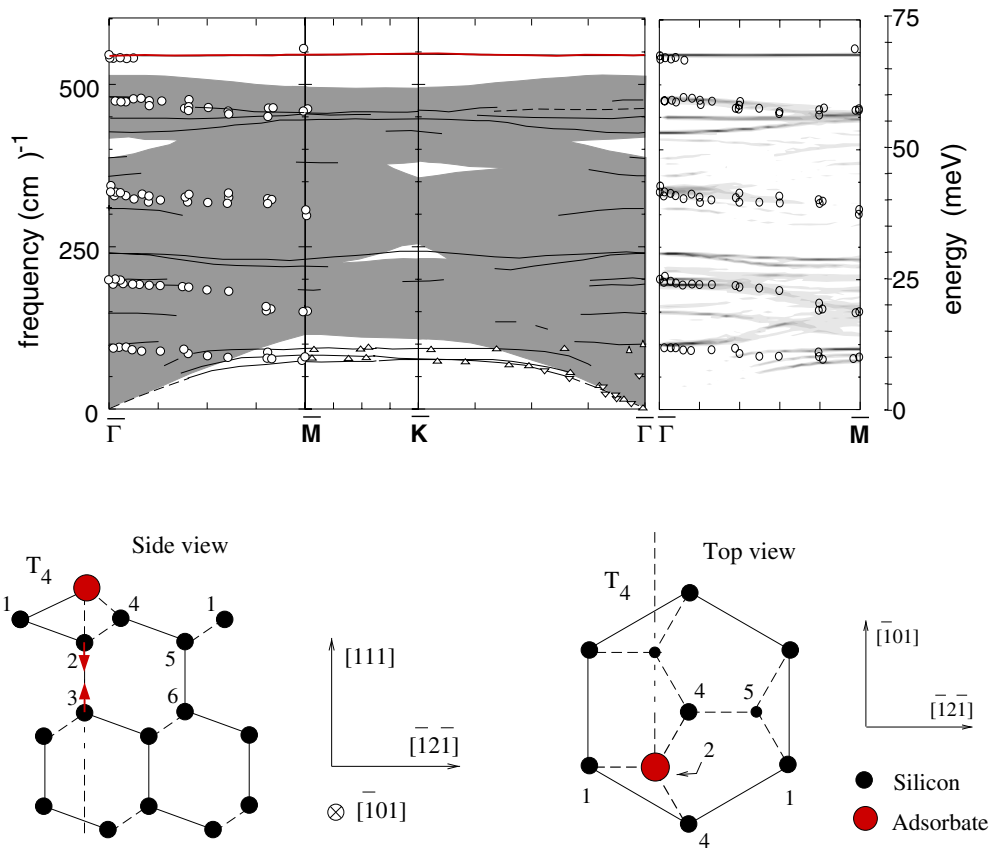

Figure 6. Phonon dispersion of Ga:Si(111)($\sqrt{3} \times \sqrt{3}$)R30° [14] and the eigenvector of the bond-stretching mode. Experimental data from inelastic helium-atom scattering [15] and high-resolution electron energy-loss spectroscopy [16] are included. The right portion of the figure illustrates an estimate for the scattering cross section computed for the $\overline{\Gamma M}$ direction.

and calculated phonon dispersion of Ga:Si(111)($\sqrt{3} \times \sqrt{3}$)R30° is a flat branch above the continuum of the bulk states, with a computed $\overline{\Gamma}$-point frequency of about 67.7 meV, which is in good agreement with the experimental value of about 68.0 meV. The corresponding eigenvector is dominated by a stretching oscillation of the compressed bond between atoms 2 and 3, which are in the second and third substrate layer and directly below the adatoms. This is illustrated in the lower portion of figure 6. The gallium atoms and the atoms in the first substrate layer are essentially at rest. The large separation of 6.74 Å between neighbouring adatoms and thus compressed bonds is reflected in a zero-dimensional behaviour of the bond-stretching mode, which has almost no dispersion.

Since the atomic and electronic structure is nearly the same for the adsorption of Al, Ga and In on Si(111), this surface mode is common for all III:Si(111)($\sqrt{3} \times \sqrt{3}$)R30° adsorption systems. Its computed vibrational energy is 68.5 meV for the subsurface stretching mode in the case of Al coverage and 67.1 meV for the coverage of Si(111) with In.

4. Phonon modes with one-dimensional signature

We now turn to cases where a surface vibrational state has constant frequency in one direction of the SBZ and shows dispersion for other directions. A simple model for this situation is illustrated in figure 7. The atoms of the linear structure are attached to the substrate by bonds with a harmonic force constant of $\varphi_{\text{on site}} = f/2$. The atoms are coupled by nearest-neighbour forces $\varphi_{\text{nn}} = f$ along the y-direction, while the interaction is zero along the x-direction. Therefore, the vibrational frequencies are constant for wavevectors along the x-axis, while the phonon branches of y-polarized modes show dispersion in the y-direction.

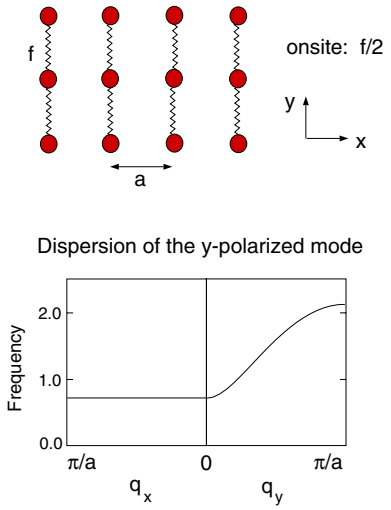

Figure 7. A spring constant model for a linear structure on a crystal surface. The atoms are allowed to oscillate in the x- and y-directions. The atoms are coupled by a nearest-neighbour force constant f along the y-direction. The on-site coupling is $f/2$.

4.1. Adsorption of Sb on III–V(110) surfaces

Antimony is an exceptionally well-behaved adsorbate for covering (110) surfaces of III–V compound semiconductors with a group-V element. The chemisorption leads to the epitaxial continued-layer (ECL) structure. In the ECL geometry, two Sb atoms are adsorbed per (1×1) unit cell of the pristine surface, occupying all atomic positions of the first missing layer derived from the symmetry of the underlying material. This is illustrated in figure 8. As a consequence of the bonding structure of the substrate, the adatoms form zigzag chains along the $[1\bar{1}0]$ direction. Each Sb atom is coupled by covalent bonds to two adatoms in the same chain and to one atom of the substrate. Interaction between two Sb–Sb chains is mediated by small long-range forces and indirectly through the interaction with the substrate.

The coupling of two Sb–Sb zigzag chains is particularly small for vibrational modes that are polarized along the chain direction and mainly localized in the adsorption layer. This is the case for the vibrational mode with a computed $\overline{\Gamma}$-point energy of 19.7, 20.9, 18.7, and 19.4 meV for Sb adsorbed on the (110) surfaces of GaAs, GaP, InAs, and InP (see figure 9). The eigenvector of this mode, which is illustrated in the lower part of the figure, is characterized by an opposing motion of neighbouring Sb atoms along the chains for all wavevectors along the $\overline{\Gamma X'}$ direction of the SBZ. In this direction, which is perpendicular to the orientation of the

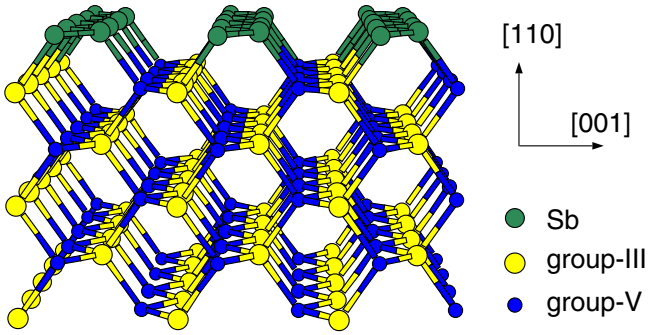

Figure 8. Adsorption of Sb on the (110) surfaces of III–V compounds into the epitaxial continued-layer structure.

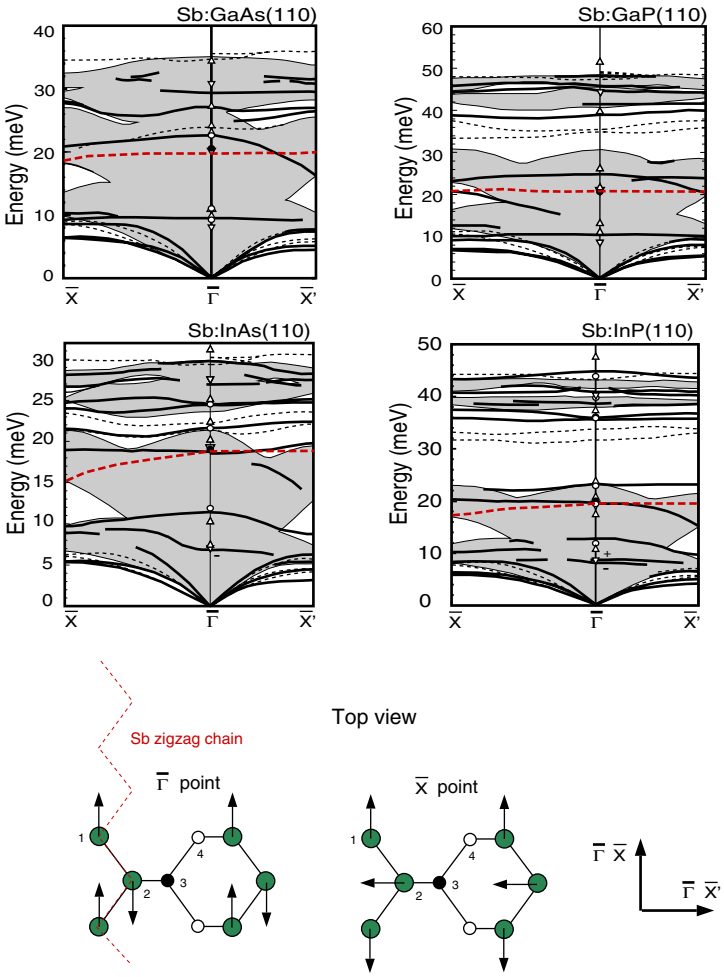

Figure 9. Phonon dispersion of Sb adsorbed on the (110) surfaces of GaAs, GaP, InAs and InP [17]. Light broken lines indicate the dispersion of selected modes of the clean surfaces. The heavy broken lines show the shear mode of the adlayer zigzag chains illustrated for the $\overline{\Gamma}$ and $\overline{X}$ point in the lower portion. Dots and triangles represent the results from Raman scattering [18–20] and another density-functional calculation [21].

chains, the related phonon branches do not show dispersion. In the $\overline{\Gamma X}$ direction, however, the frequency is notably reduced to lower vibrational energies, particularly in the case of Sb:InAs(110), while the simple model shown in figure 7 gives an increase of the frequency. The reason for this is that the zigzag bonding structure in the chains couples x- and y-polarized displacements. For wavevectors of the $\overline{\Gamma X}$ direction, it is not forbidden by symmetry that the eigenvectors have vibrations along and perpendicular to the chains. By this it is possible to reduce bond-stretching forces in the chains.

4.2. Dimer rows on Si(001)(2×1)

It is generally accepted that the basic reconstruction of the Si(001) surface consists in the formation of dimers arranged in rows perpendicular to the dimer bonding direction (see figure 10). The resulting p(2×1) structure has clearly been resolved by STM [1]. Buckling of the dimers reduces the surface energy. Highly converged *ab initio* calculations achieve an energy gain per dimer of about 0.1 eV for the asymmetric configuration compared to the symmetric case. The formation of dimer rows indicates that the interaction of first-layer Si atoms is large in the direction of the rows and small between neighbouring rows of dimers.

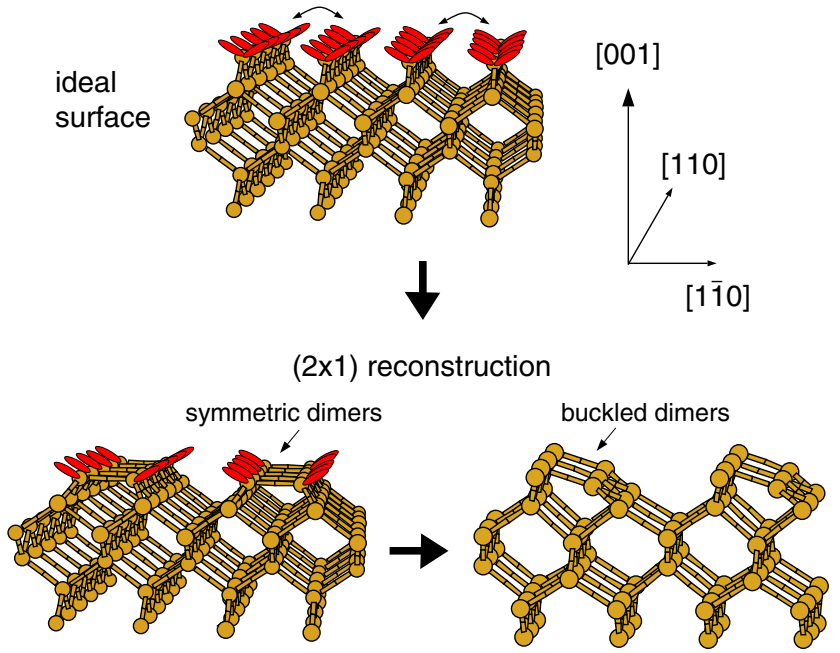

Figure 10. Reconstruction of Si(001) into the (2×1) buckled dimer geometry. Dimers formed between neighbouring first-layer atoms are aligned in rows which are oriented perpendicular to the dimer bonding direction. Buckling of the dimers reduces the surface energy.

A fingerprint of the dimer reconstruction is the rocking mode illustrated in the lower part of figure 11. It is characterized by an opposing up and down displacement of the surface atoms leading to a rocking motion of the dimers increasing and decreasing periodically the tilt angle. This mode's phonon branch is almost flat along the $\overline{\Gamma J}$ and $\overline{KJ'}$ directions. This shows that the interaction between neighbouring dimer rows is weak. The wavevector component

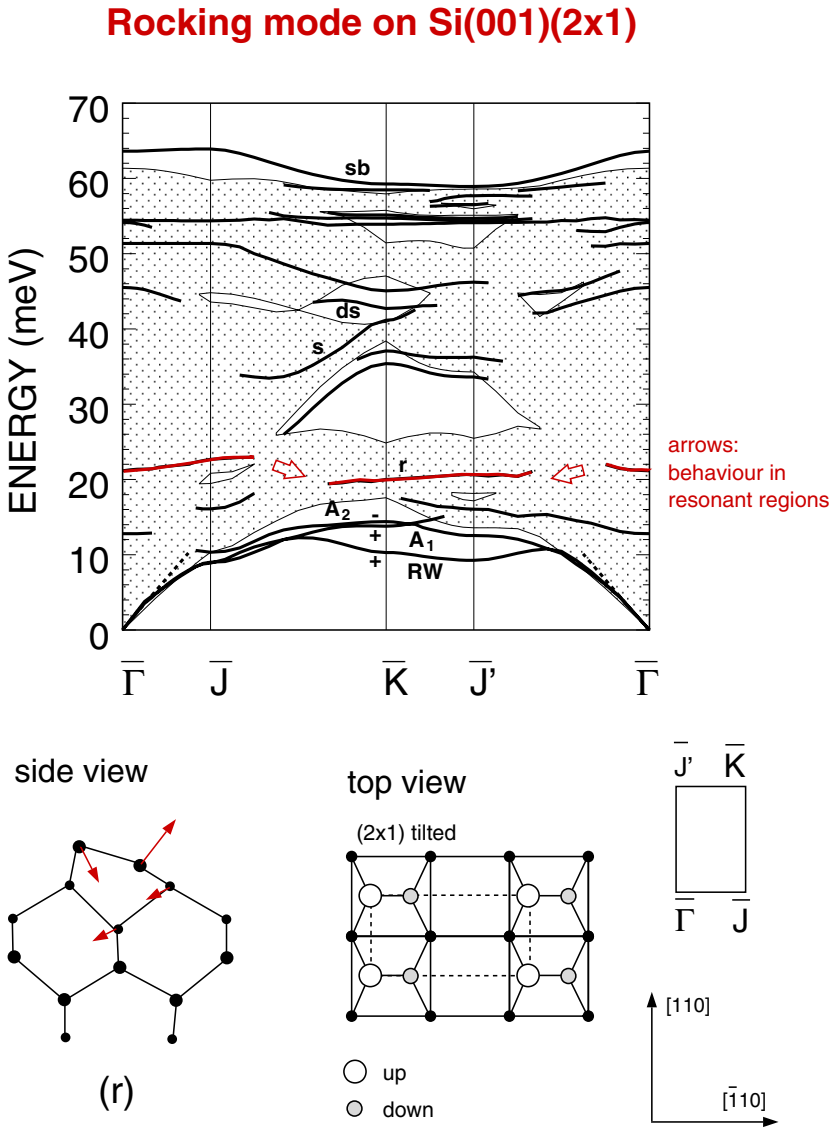

Figure 11. Phonon dispersion of the tilted-dimer Si(001)p(2 × 1) surface [22]. The rocking mode (r) illustrated in the side view is a fingerprint of the buckled dimer structure.

along the rows changes along the $\overline{\mathrm{JK}}$ and $\overline{\Gamma \mathrm{J}'}$ directions. Hence, the appreciable variation of the rocking-mode frequency indicated by the arrows in figure 11 reflects the coupling of the dimers along a row. The resonant behaviour also reveals substantial coupling of the rocking vibration with bulk phonon modes.

5. Surface phonons with usual dispersion

The majority of the surface phonon branches illustrated in figures 3, 5, 9, and 11 show dispersion in all directions of the SBZ. This is in particular the case for surface acoustic waves,

which are characterized by a linear increase of their vibrational energy close to the $\overline{\Gamma}$ point. In the limit of small wavevectors, surface acoustic waves depend only on elastic constants and other macroscopic properties of the material. They are solutions of the equations of motion in the continuum limit, taking into account the boundary conditions introduced by the truncation of the solid at the surface, which can be treated as a two-dimensional plane. Well-known representatives of surface acoustic waves are the Rayleigh waves [23] and their generalized version. These and all other macroscopic vibrational modes penetrate deeply into bulk layers. They can be derived from macroscopic properties of the material and are insensitive to structural details of the surface, as long as their wavelength is large enough. For the Sb-covered III–V(110) surfaces, three acoustic phonon modes appear in the $\overline{\Gamma X}$ direction, while two or three such branches are seen along the $\overline{\Gamma X'}$ direction.

Also most of the true or so-called microscopic surface vibrational modes have dispersion in all directions of the SBZ. Figure 12 shows displacement patterns of two selected vibrational states of Sb:InP(110). The mode being illustrated in the upper part of the figure lies above the continuum of the surface-projected bulk bands of InP. Its dispersion in the $\overline{\Gamma X'}$ direction originates in an interaction of the oscillating substrate atoms mediated by the adsorption layer. The energies of the gap mode illustrated in the lower portion of the figure are 35.8 and 36.7 meV at the $\overline{\Gamma}$ and $\overline{X'}$ points, respectively. The coupling in the [001] direction originates in the deformation of the sixfold rings defined by the substrate atoms and adlayer atoms.

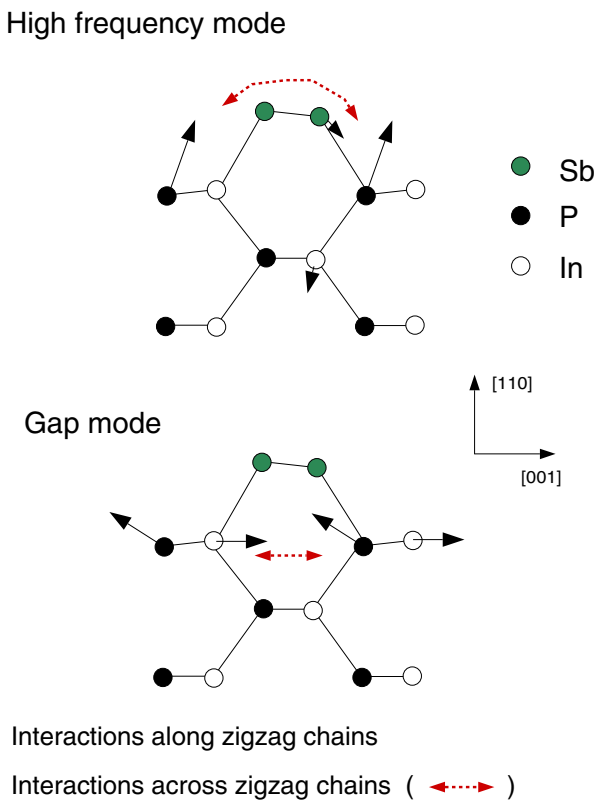

Figure 12. The displacement pattern of two microscopic modes of Sb:InP(110) which show dispersion along and across the Sb–Sb surface chains. The eigenvectors are shown for the $\overline{\Gamma}$ point of the SBZ.

6. Summary

Phonon dispersion curves of semiconductor surfaces were discussed in terms of signatures for zero- and one-dimensional structures, which can be the result of atomic rearrangements, rebonding, or adsorption. Usual surface phonon modes change their frequency with varying wavevector along all directions of the SBZ. Vibrational states of linear structures on a surface, however, change their energy only with a variation of the wavevector component along the structures' orientation. Examples are the shear modes of the adlayer zigzag chains of Sb chemisorbed on the (110) surfaces of III–V compound semiconductors and the rocking mode of the Si(001)p(2×1) surface. Structures with zero-dimensional character can result from the adsorption of small atoms like hydrogen or by low-coverage chemisorption of larger atoms. In this context, the hydrogen stretching modes of H:Si(111)(1×1) and the subsurface bond-stretching mode of the III:Si(111)($\sqrt{3} \times \sqrt{3}$)R30° surface were discussed.

The atomic equilibrium positions, charge redistribution, and rebonding are the main factors that determine interatomic force constants and thereby the phonon mode frequencies. Hence, the given examples show that a careful analysis of surface phonon dispersion curves can provide useful and important information about the structure of crystal surfaces. The three main experimental techniques currently available to measure surface phonon dispersion curves are inelastic helium-atom scattering, high-resolution electron energy-loss spectroscopy, and Raman spectroscopy. With helium-atom scattering it is difficult to measure vibrational frequencies above 20 meV. The resolution of electron energy-loss spectroscopy is limited. Raman spectroscopy allows one to probe essentially only zone-centre phonon modes. It is therefore desirable to develop further experimental techniques for the measurement of surface phonon dispersion curves. Already, synchrotron radiation is used in x-ray standing-wave [24] and grazing-incidence diffraction experiments [25] to determine atomic positions in the surface region. As for the measurement of bulk phonon dispersion curves with synchrotron radiation, one may expect the successful application of inelastic x-ray scattering at crystal surfaces in the future.

References

[1] Hamers R J, Tromp R M and Demuth J E 1986 *Phys. Rev.* B **34** 5343
[2] Feenstra R M, Stroscio J A, Tersoff J and Fein A P 1987 *Phys. Rev. Lett.* **58** 1192
[3] Hohenberg P and Kohn W 1964 *Phys. Rev.* **136** B864
[4] Kohn W and Sham L J 1965 *Phys. Rev.* **140** A1133
[5] Baroni S, Giannozzi P and Testa A 1987 *Phys. Rev. Lett.* **58** 1861
[6] Giannozzi P, de Gironcoli S, Pavone P and Baroni S 1991 *Phys. Rev.* B **43** 7231
[7] Pavone P 2001 *J. Phys.: Condens. Matter* **13**
[8] Chabal Y J, Dumas P, Guyout-Sionnest P and Higashi G S 1991 *Surf. Sci.* **242** 524
[9] Honke R, Pavone P and Schröder U 1996 *Surf. Sci.* **367** 75
[10] Stuhlmann C, Bogdányi G and Ibach H 1992 *Phys. Rev.* B **45** 6786
[11] Hamers R J 1989 *Phys. Rev.* B **40** 1657
[12] Nogami J, Park S-i and Quate C F 1988 *Surf. Sci.* **203** L631
[13] Zegenhagen J, Patel J R, Freeland P, Chen D M, Golovchenko J A, Bedrossian P and Northrup J E 1989 *Phys. Rev.* B **39** 1298
[14] Eckl C, Honke R, Fritsch J, Pavone P and Schröder U 1997 *Z. Phys.* B **104** 715
[15] Doak R B 1989 *J. Vac. Sci. Technol.* B **7** 1252
[16] Schmidt J, Ibach H and Müller J E 1995 *Phys. Rev.* B **51** 5233
[17] Fritsch J, Arnold M and Schröder U 2000 *Phys. Rev.* B **61** 16 682
[18] Hünermann M 1990 *PhD Thesis* Aachen University of Technology, Germany
Hünermann M, Geurts L and Richter W 1991 *Phys. Rev. Lett.* **66** 640
[19] Richter W, Esser N, Kelnberger A and Köpp M 1992 *Solid State Commun.* **84** 165

[20] Esser N, Köpp M, Haier P and Richter W 1995 *Phys. Status Solidi* a **152** 191
[21] Schmidt W G and Srivastava G P 1995 *Surf. Sci.* **331–333** 540
[22] Fritsch J and Pavone P 1995 *Surf. Sci.* **344** 159
[23] Rayleigh Lord 1887 *Proc. Lond. Math. Soc.* **17** 4
[24] Woicik J C, Kendelewicz T, Miyano K E, Cowan P L, Bouldin C E, Karlin B A, Pianetta P E and Spicer W E 1992 *Phys. Rev. Lett.* **68** 341
[25] Ruocco A, Nannarone S, Sauvage-Simkin M, Jedrecy N, Pinchaux R and Waldhauer A 1994 *Surf. Sci.* **307–309** 662